Variational Laplace for Bayesian neural networks

Ali Unlu [1] **Laurence Aitchison** [2]

Abstract

We develop variational Laplace for Bayesian neural networks (BNNs) which exploits a local approximation of the curvature of the likelihood to estimate the ELBO without the need for stochastic sampling of the neural-network weights. Variational Laplace performs better on image classification tasks than MAP inference and far better than standard variational inference with stochastic sampling despite using the same mean-field Gaussian approximate posterior. The Variational Laplace objective is simple to evaluate, as it is (in essence) the log-likelihood, plus weight-decay, plus a squared-gradient regularizer. Finally, we emphasise care needed in benchmarking standard VI as there is a risk of stopping before the variance parameters have converged. We show that early-stopping can be avoided by increasing the learning rate for the variance parameters.

1. Introduction

Neural networks are increasingly being used in safety-critical settings such as self-driving cars (Bojarski et al., 2016) and medical diagnosis (Amato et al., 2013). In these settings, it is critical to be able to reason about uncertainty in the parameters of the network, for instance so that the system is able to call for additional human input when necessary (McAllister et al., 2017). Several approaches to Bayesian inference in neural networks are available, including stochastic gradient Langevin dynamics (Welling & Teh, 2011) Laplace's method (Azevedo-Filho & Shachter, 1994; MacKay, 2003; Ritter et al., 2018) and variational inference (Blundell et al., 2015; Ober & Aitchison, 2020).

Here, we focus on combining the advantages of Laplace's method (Azevedo-Filho & Shachter, 1994; MacKay, 2003; Ritter et al., 2018) and variational inference (VI; Wainwright & Jordan, 2008). In particular, Laplace's method is very fast as it begins by finding a mode using a standard gradient descent procedure, then computes a local Gaussian approximate of the mode by performing a second-order Taylor expansion. However, as the mode is discovered by standard gradient descent, it may be a narrow mode that generalises poorly (Neyshabur et al., 2017). In contrast, variational inference (VI; Blundell et al., 2015) is slower as it requires stochastic sampling of the weights, but that stochastic sampling forces it to find a broad, flat mode that presumably generalises better. Here, we develop a new Variational Laplace (VL) method that combines the best of both methods, giving a method that finds broad, flat modes even in the absence of the stochastic sampling. The resulting objective is composed of the log-likelihood, standard weight-decay regularization and a squared-gradient regularizer, which is weighted by the variance of the approximate posterior. VL displayed improved performance over VI and MAP on standard benchmark tasks for fixed and learned variance approximate posteriors.

[1]Department of Infomatics, University of Sussex, Brighton, UK [2]Department of Computer Science, University of Bristol, Bristol, UK. Correspondence to: Laurence Aitchison <laurence.aitchison@gmail.com>.

2. Background

2.1. Variational inference (VI) for Bayesian neural networks

To perform Variational Inference for neural networks, we follow the usual convention (Blundell et al., 2015), in using independent Gaussian priors, P and approximate posteriors Q for all parameters, $\mathbf{w}$,

$$\mathrm{P}\left(w_\lambda\right) = \mathcal{N}\left(w_\lambda; 0, s_\lambda^2\right) \tag{1}$$

$$\mathrm{Q}\left(w_\lambda\right) = \mathcal{N}\left(w_\lambda; \mu_\lambda, \sigma_\lambda^2\right) \quad \text{equivalently} \tag{2}$$

$$\mathrm{Q}\left(\mathbf{w}\right) = \mathcal{N}\left(\mathbf{w}; \boldsymbol{\mu}, \boldsymbol{\Sigma}\right), \tag{3}$$

where μ_λ and σ_λ^2 are learned parameters of the approximate posterior, and where $\boldsymbol{\Sigma}$ is a diagonal matrix, with $\Sigma_{\lambda\lambda} = \sigma_\lambda^2$. We fit the approximate posterior by optimizing the evidence lower bound objective (ELBO) with respect to parameters of the variational posterior, μ_λ and σ_λ^2, using the reparameterisation trick (Appendix A),

$$\mathcal{L}_{\mathrm{VI}} = \mathop{\mathbb{E}}_{\mathrm{Q}(\mathbf{w})}\left[\log \mathrm{P}\left(\mathbf{y}|\mathbf{x}, \mathbf{w}\right) + \beta \log \frac{\log \mathrm{P}\left(\mathbf{w}\right)}{\log \mathrm{Q}\left(\mathbf{w}\right)}\right]. \tag{4}$$

Here, $\mathbf{x}$ is all training inputs, $\mathbf{y}$ is all training outputs, and β is the tempering parameter which is 1 for a close approximation to Bayesian inference, but is often set to smaller

values to "temper" the posterior, which often improves empirical performance (Huang et al., 2018; Wenzel et al., 2020) and has theoretical justification as accounting for the data-curation process (Aitchison, 2020).

2.2. Laplace's method

Laplace's method (Azevedo-Filho & Shachter, 1994; MacKay, 2003; Ritter et al., 2018) first finds a mode by doing gradient ascent on the log-joint,

$$\mathbf{w}^* = \arg\max_{\mathbf{w}} \left[\log \mathrm{P}\left(\mathbf{y}|\mathbf{x}, \mathbf{w}\right) + \log \mathrm{P}\left(\mathbf{w}\right)\right] \tag{5}$$

and uses a Gaussian approximate posterior around that mode,

$$\mathrm{Q}\left(\mathbf{w}\right) = \mathcal{N}\left(\mathbf{w}; \mathbf{w}^*, -\mathbf{H}^{-1}(\mathbf{w}^*)\right) \tag{6}$$

where $\mathbf{H}(\mathbf{w}^*)$ is Hessian of the log-joint at $\mathbf{w}^*$.

3. Related work

There is past work on Variational Laplace (Friston et al., 2007; Daunizeau et al., 2009; Daunizeau, 2017), which learns the mean parameters, $\boldsymbol{\mu}$, of a Gaussian approximate posterior,

$$\mathrm{Q}_{\boldsymbol{\mu}}\left(\mathbf{w}\right) = \mathcal{N}\left(\mathbf{w}; \boldsymbol{\mu}, -\mathbf{H}^{-1}(\boldsymbol{\mu})\right) \tag{7}$$

and obtains the covariance matrix as a function of the mean parameters using the Hessian, as in Laplace's method. However, instead of taking the approximation to be centered around a MAP solution, $\mathbf{w}^*$, they take the approximate posterior to be centered on learned mean parameters, $\boldsymbol{\mu}$. Importantly, they simplify the ELBO by substituting this approximate posterior (Eq. 4), and approximating the log-joint using its Taylor series expansion. Ultimately they obtain,

$$\begin{aligned}\mathcal{L}_{\mathrm{VI}} \approx \log \mathrm{P}\left(\mathbf{y}|\mathbf{w}{=}\boldsymbol{\mu}, \mathbf{x}\right) + \log \mathrm{P}\left(\mathbf{w}{=}\boldsymbol{\mu}\right) \\ - \tfrac{1}{2} \log |\mathbf{H}(\boldsymbol{\mu})| + \text{const.}\end{aligned} \tag{8}$$

However, this approach is problematic for three reasons. First, the Hessian is not always negative definite, and may even be singular, in which case the objective is undefined. Second, the algebraic manipulations required to derive Eq. (8) require the full $N \times N$ Hessian, $\mathbf{H}(\boldsymbol{\mu})$, for all N parameters, and neural networks have too many parameters for this to be feasible. Third, the $\log |\mathbf{H}(\boldsymbol{\mu})|$ term in Eq. (8) cannot be minibatched, as we need the full sum over minibatches inside the $\log$ to compute the Hessian,

$$\log |\mathbf{H}(\boldsymbol{\mu})| = \log \left|\textstyle\sum_j \mathbf{H}_j(\boldsymbol{\mu})\right|, \tag{9}$$

where $\mathbf{H}_j(\boldsymbol{\mu})$ is the contribution to the Hessian from an individual minibatch. Due to these issues, past work on Variational Laplace was not able to apply the method to large-scale neural networks.

An alternative deterministic approach to variational inference in Bayesian neural networks, approximates the distribution over activities induced by stochasticity in the weights (Wu et al., 2018) as a Gaussian. Unfortunately, it is potentially important to capture the covariance over features induced by stochasticity in the weights. In fully connected networks, this is feasible, as we usually have a small number of features at each layer. However, in convolutional networks, we have a large number of features, $\texttt{channels} \times \texttt{height} \times \texttt{width}$. In the lower layers of a ResNet, we may have 64 channels and a 32×32 feature map, resulting in $64 \times 32^2 = 65,536$ features and a $65,536 \times 65,536$ covariance matrix. These scalability issues prevented them from applying their approach to convolutional networks. In contrast, our approach is highly scalable and readily applicable in the convolutional setting.

Ritter et al. (2018) used Laplace's method in Bayesian neural networks, by first finding the mode by doing gradient ascent on the log-joint probability, and expanding around that mode. As usual for Laplace's method, they risk finding a narrow mode that generalises poorly. In contrast, we find a mode using an approximation to the ELBO that takes the curvature into account and hence is biased towards broad, flat modes that presumably generalise better.

Finally, our approach will eventually give a squared-gradient regularizer that is similar to those discovered in past work (Barrett & Dherin, 2020; Smith et al., 2021). This work found a slightly different squared-gradient regularizer has a connection to gradient descent, in that approximation errors due to finite-step sizes in gradient-descent imply an effective squared gradient regularization. The similarity of our objectives raises profound questions about the extent to which gradient descent can be said to perform Bayesian inference. That said there are two key differences. First, our method uses the Fisher, i.e. the gradients for data sampled from the model, whereas their approach uses the empirical Fisher, i.e. gradients for the observed data to form the squared gradient regularizer (Kunstner et al., 2019). Second, our approach gives a principled method to learn the weight for the squared-gradient regularizer for each parameter separately, whereas the connection to SGD forces Barrett & Dherin (2020) to use a uniform weight across all parameters.

4. Methods

To combine the best of VI and Laplace's method, we begin by noting that the ELBO can be rewritten in terms of the KL

divergence between the prior and approximate posterior,

$$\mathcal{L}_{\text{VI}} = \mathop{\mathbb{E}}_{\text{Q}(\mathbf{w})}\left[\log \text{P}\left(\mathbf{y}|\mathbf{x},\mathbf{w}\right)\right] - \beta\textstyle\sum_\lambda \text{D}_{\text{KL}}\left(\text{Q}\left(w_\lambda\right)||\,\text{P}\left(w_\lambda\right)\right), \quad (10)$$

where the KL-divergence can be evaluated analytically,

$$D_{\text{KL}}\left(\text{Q}\left(w_\lambda\right)||\,\text{P}\left(w_\lambda\right)\right) = \frac{1}{2}\left(\frac{\sigma_\lambda^2+\mu_\lambda^2}{s_\lambda^2} - 1 + \log\frac{s_\lambda^2}{\sigma_\lambda^2}\right). \quad (11)$$

As such, the only term we need to approximate is the expected log-likelihood.

To approximate the expectation, we begin by taking a second-order Taylor series expansion of the log-likelihood around the current setting of the mean parameters, $\boldsymbol{\mu}$,

$$\begin{aligned}\mathop{\mathbb{E}}_{\text{Q}(\mathbf{w})}\left[\log \text{P}\left(\mathbf{y}|\mathbf{x},\mathbf{w}\right)\right] &\approx \log \text{P}\left(\mathbf{y}|\mathbf{x},\mathbf{w}{=}\boldsymbol{\mu}\right) \\ &+ \mathop{\mathbb{E}}_{\text{Q}(\mathbf{w})}\left[\textstyle\sum_{j=1}^B \mathbf{g}_j^T\left(\mathbf{w}-\boldsymbol{\mu}\right)\right] \quad (12)\\ &+ \mathop{\mathbb{E}}_{\text{Q}(\mathbf{w})}\left[\tfrac{1}{2}\left(\mathbf{w}-\boldsymbol{\mu}\right)^T\mathbf{H}\left(\mathbf{w}-\boldsymbol{\mu}\right)\right]\end{aligned}$$

where B is the number of minibatches, $\mathbf{g}_j$ is the gradient for minibatch j and $\mathbf{H}$ is the Hessian for the full dataset,

$$g_{j;\lambda} = \frac{\partial}{\partial w_\lambda}\left[\log \text{P}\left(\mathbf{y}_j|\mathbf{x}_j,\mathbf{w}\right)\right] \quad (13)$$

$$H_{\lambda,\nu} = \frac{\log \text{P}\left(\mathbf{y}|\mathbf{x},\mathbf{w}\right)}{\partial w_\lambda \partial w_\nu} \quad (14)$$

where $\mathbf{x}$ and $\mathbf{y}$ are the the inputs and outputs for the full dataset, whereas $\mathbf{x}_j$ and $\mathbf{y}_j$ are the inputs and outputs for minibatch j. Now we consider the expectation of each of these terms under the approximate posterior, $\text{Q}\left(\mathbf{w}\right)$. The first term is constant and independent of $\mathbf{w}$. The second (linear) term is zero, because the expectation of $\left(\mathbf{w}-\boldsymbol{\mu}\right)$ under the approximate posterior is zero

$$\mathop{\mathbb{E}}_{\text{Q}(\mathbf{w})}\left[\mathbf{g}_j^T\left(\mathbf{w}-\boldsymbol{\mu}\right)\right] = \mathbf{g}_j^T\mathop{\mathbb{E}}_{\text{Q}(\mathbf{w})}\left[\left(\mathbf{w}-\boldsymbol{\mu}\right)\right] = \mathbf{0} \quad (15)$$

the third (quadratic) term might at first appear difficult to evaluate because it involves $\mathbf{H}$, the $N\times N$ matrix of second derivatives, where N is the number of parameters in the model. However, using properties of the trace, and noting that the expectation of $\left(\mathbf{w}-\boldsymbol{\mu}\right)\left(\mathbf{w}-\boldsymbol{\mu}\right)^T$ is the covariance of the approximate posterior we obtain,

$$\begin{aligned}&\mathop{\mathbb{E}}_{\text{Q}(\mathbf{w})}\left[\tfrac{1}{2}(\mathbf{w}-\boldsymbol{\mu})^T\mathbf{H}(\mathbf{w}-\boldsymbol{\mu})\right]\\ &\quad= \mathop{\mathbb{E}}_{\text{Q}(\mathbf{w})}\left[\tfrac{1}{2}\,\text{Tr}\left(\mathbf{H}\left(\mathbf{w}-\boldsymbol{\mu}\right)\left(\mathbf{w}-\boldsymbol{\mu}\right)^T\right)\right]\\ &\quad= \tfrac{1}{2}\,\text{Tr}\left(\mathbf{H}\boldsymbol{\Sigma}\right) \quad (16)\end{aligned}$$

writing the trace in index notation, and substituting for the (diagonal) posterior covariance, $\boldsymbol{\Sigma}$,

$$\tfrac{1}{2}\,\text{Tr}\left(\mathbf{H}\boldsymbol{\Sigma}\right) = \tfrac{1}{2}\sum_{\lambda\nu} H_{\lambda\nu}\Sigma_{\lambda\nu} = \tfrac{1}{2}\sum_\lambda H_{\lambda\lambda}\sigma_\lambda^2 \quad (17)$$

Thus, our first approximation of the expected log-likelihood is,

$$\mathop{\mathbb{E}}_{\text{Q}(\mathbf{w})}\left[\log \text{P}\left(\mathbf{y}|\mathbf{x},\mathbf{w}\right)\right] \approx \log \text{P}\left(\mathbf{y}|\mathbf{x},\mathbf{w}{=}\boldsymbol{\mu}\right) + \tfrac{1}{2}\textstyle\sum_\lambda \sigma_\lambda^2 H_{\lambda\lambda} \quad (18)$$

And substituting this into Eq. (10) gives,

$$\mathcal{L}_{\text{VI}} \approx \mathcal{L}_{\text{VL(H)}} = \log \text{P}\left(\mathbf{y}|\mathbf{x},\mathbf{w}{=}\boldsymbol{\mu}\right) + \tfrac{1}{2}\textstyle\sum_\lambda \sigma_\lambda^2 H_{\lambda\lambda} - \beta\textstyle\sum_\lambda \text{D}_{\text{KL}}\left(\text{Q}\left(w_\lambda\right)||\,\text{P}\left(w_\lambda\right)\right). \quad (19)$$

This resolves most of the issues with the original Variational Laplace method: it requires only the diagonal of the Hessian, it can be minibatched and it does not blow up if $H_{\lambda\lambda}$ is zero.

4.1. Pathological optima when using the Hessian

However, a new issue arises: $H_{\lambda\lambda}$ is usually negative, in which case we the approximation in Eq. (19) can be expected to work well. However there is nothing to stop $H_{\lambda\lambda}$ from becoming positive, and if it does, we may get pathological optimal values of σ_λ^2. In particular, picking out the terms in the objective that depend on σ_λ^2 (and putting the others into const) and taking $\beta = 1$ for simplicity, we have

$$\mathcal{L}_{\text{VL(H)}} = \tfrac{1}{2}\textstyle\sum_\lambda\left(-\left(\frac{1}{s_\lambda^2} - H_{\lambda\lambda}\right)\sigma_\lambda^2 + \log\sigma_\lambda^2\right) + \text{const.} \quad (20)$$

Thus, the gradient wrt a single variance parameter is,

$$\frac{\partial}{\partial\sigma_\lambda^2}\mathcal{L}_{\text{VL(H)}} = \tfrac{1}{2}\left(-\left(\frac{1}{s_\lambda^2} - H_{\lambda\lambda}\right) + \frac{1}{\sigma_\lambda^2}\right). \quad (21)$$

In the typical case, $H_{\lambda\lambda}$ is negative so $\left(\frac{1}{s_\lambda^2} - H_{\lambda\lambda}\right)$ is positive, and we can find the optimum by solving for the value of σ_λ^2 where the gradient is zero,

$$\sigma_\lambda^2 = \frac{1}{\frac{1}{s_\lambda^2} - H_{\lambda\lambda}} \quad (22)$$

However, if $H_{\lambda\lambda}$ is positive and sufficiently large, $H_{\lambda\lambda} > \frac{1}{s_\lambda^2}$, then $\left(\frac{1}{s_\lambda^2} - H_{\lambda\lambda}\right)$ becomes negative, and not only is the mode in Eq. (22) undefined, but the gradient is always positive,

$$0 < \frac{\partial}{\partial\sigma_\lambda^2}\mathcal{L}_{\text{VL(H)}} = \tfrac{1}{2}\left(-\left(\frac{1}{s_\lambda^2} - H_{\lambda\lambda}\right) + \frac{1}{\sigma_\lambda^2}\right). \quad (23)$$

as both terms in the sum: $-\left(\frac{1}{s_\lambda^2} - H_{\lambda\lambda}\right)$ and $\frac{1}{\sigma_\lambda^2}$ are positive. As such, when $H_{\lambda\lambda} > \frac{1}{s_\lambda^2}$, the variance, σ_λ^2 grows without bound.

4.2. Avoiding pathologies with the Fisher

To avoid pathologies arising from the fact that the Hessian is not necessarily negative definite, a common approach is to approximate the Hessian using the Fisher Information matrix,

$$-\mathbf{H} \approx \mathbf{F} = \sum_{j=1}^{B} \mathop{\mathbb{E}}_{\mathrm{P}(\tilde{\mathbf{y}}_j|\mathbf{x}_j,\mathbf{w}=\boldsymbol{\mu})} \left[\tilde{\mathbf{g}}_j(\tilde{\mathbf{y}}_j)\tilde{\mathbf{g}}_j^T(\tilde{\mathbf{y}}_j)\right]. \quad (24)$$

Importantly, $\tilde{\mathbf{g}}$ is the gradient of the log-likelihood for data sampled from the model, $\tilde{\mathbf{y}}_j$, *not* for the true data,

$$\tilde{g}_{j;\lambda}(\tilde{\mathbf{y}}_j) = \frac{\partial}{\partial w_\lambda}\left[\log \mathrm{P}\left(\tilde{\mathbf{y}}_j|\mathbf{x}_j,\mathbf{w}\right)\right]. \quad (25)$$

This gives us the Fisher, which is a commonly used and well-understood approximation to the Hessian (Kunstner et al., 2019). Importantly, this contrasts with the empirical Fisher (Kunstner et al., 2019), which uses the gradient conditioned on the actual data (and not data sampled from the model),

$$\mathbf{F}_{\text{emp}} = \sum_{j=1}^{B} \mathbf{g}_j \mathbf{g}_j^T, \quad (26)$$

which is problematic, because there is a large rank-1 component in the direction of the mean gradient, which disrupts the estimated matrix specifically in the direction of interest for problems such as optimization (Kunstner et al., 2019).

Using the Fisher Information (Eq. 24) in Eq. (18), we obtain an approximate lower-bound on the expected log-likelihood,

$$\mathop{\mathbb{E}}_{\mathrm{Q}(\mathbf{w})}\left[\log \mathrm{P}\left(\mathbf{y}|\mathbf{x},\mathbf{w}\right)\right] \approx \log \mathrm{P}\left(\mathbf{y}|\mathbf{x},\mathbf{w}=\boldsymbol{\mu}\right) - \tfrac{1}{2}\textstyle\sum_\lambda \sigma_\lambda^2 \sum_{j=1}^{B} \tilde{g}_{j;\lambda}^2 \quad (27)$$

Substituting this into Eq. (10) gives us the final VL objective, $\mathcal{L}_{\text{VL}}$, which forms an approximate lower-bound on the ELBO,

$$\mathcal{L}_{\text{VI}} \approx \mathcal{L}_{\text{VL}} = \log \mathrm{P}\left(\mathbf{y}|\mathbf{x},\mathbf{w}=\boldsymbol{\mu}\right) - \tfrac{1}{2}\textstyle\sum_\lambda \sigma_\lambda^2 \sum_{j=1}^{B} \tilde{g}_{j;\lambda}^2 - \beta \textstyle\sum_\lambda \mathrm{D}_{\text{KL}}\left(\mathrm{Q}\left(w_\lambda\right) || \, \mathrm{P}\left(w_\lambda\right)\right). \quad (28)$$

In practice, we typically take the objective for a minibatch, divided by the number of datapoints in a minibatch, S,

$$\tfrac{1}{S}\mathcal{L}_{\text{VL};j} = \tfrac{1}{S}\log \mathrm{P}\left(\mathbf{y}_j|\mathbf{x}_j,\mathbf{w}=\boldsymbol{\mu}\right) - \tfrac{S}{2}\textstyle\sum_\lambda \sigma_\lambda^2 \left(\tfrac{1}{S}\tilde{g}_{j;\lambda}\right)^2 - \tfrac{\beta}{2SB}\textstyle\sum_\lambda \left(\tfrac{\sigma_\lambda^2+\mu_\lambda^2}{s_\lambda^2} - 1 + \log \tfrac{s_\lambda^2}{\sigma_\lambda^2}\right). \quad (29)$$

where $\left(\frac{1}{S}\tilde{g}_{j;\lambda}\right)$ are the gradients of the log-likelihood for the minibatch averaged across datapoints, i.e. the gradient of $\frac{1}{S}\log \mathrm{P}\left(\tilde{\mathbf{y}}_j|\mathbf{x}_j,\mathbf{w}=\boldsymbol{\mu}\right)$. Remember B is the number of minibatches so SB is the total number of training datapoints.

4.3. Constraints on the network architecture

Importantly, here the regularizer is the squared gradient of the loss with respect to the parameters. As such, computing the loss implicitly involves a second-derivative of the log-likelihood, and we therefore cannot use piecewise linear activation functions such as ReLU, which have pathological second derivatives. Instead, we used a softplus activation function, but any activation with well-behaved second derivatives is admissible.

5. Results

We trained a PreactResNets-18 (He et al., 2016) on various datasets using the Adam optimizer (Kingma & Ba, 2014), with an initial learning rate of 1E-4, which decreased by a factor of 10 after 100 and 150 epochs and a batch size of 128 with all the other optimizer hyperparameters set to their default values. In many resource-constrained settings it is important to be able to use a representative neural-network to make predictions, rather than needing to run the inputs through many samples from a posterior (e.g. Malinin et al., 2019). As such, and for a fair comparison against MAP inference, we used a single network at the mean parameters for both VI and VL.

5.1. Fixed variance

We began by comparing VL with VI for isotropic Gaussian approximate posteriors with fixed variances (Fig. 1). This is an interesting setting both because it eliminates difficulties with estimating those variances in VI (see Sec. 5.2 below), and because these posteriors have interesting connections to the isotropic Gaussian stationary distributions of SGD in quadratic objectives (Appendix B). These stationary distributions have variance,

$$\sigma^2 = \frac{\eta_{\text{SGD}}}{2S_{\text{SGD}}} \quad (30)$$

where η_{SGD} is the SGD learning rate and S_{SGD} is the SGD batch size. This is closely related to VI approximate posteriors with fixed-variance approximate posteriors. With such fixed-variance approximate posteriors, VL shows considerably improved performance over both MAP and VI, especially at larger approximate posterior variances (Fig. 2).

5.2. Early-stopping and poor performance in VI

Before performing comparisons where we learn the approximate posterior variance, it is important to understand the pitfalls when optimizing variational Bayesian neural networks using adaptive optimizers such as Adam. In particular, there is a strong danger of stopping the optimization before the variances have converged. To illustrate this risk, note that

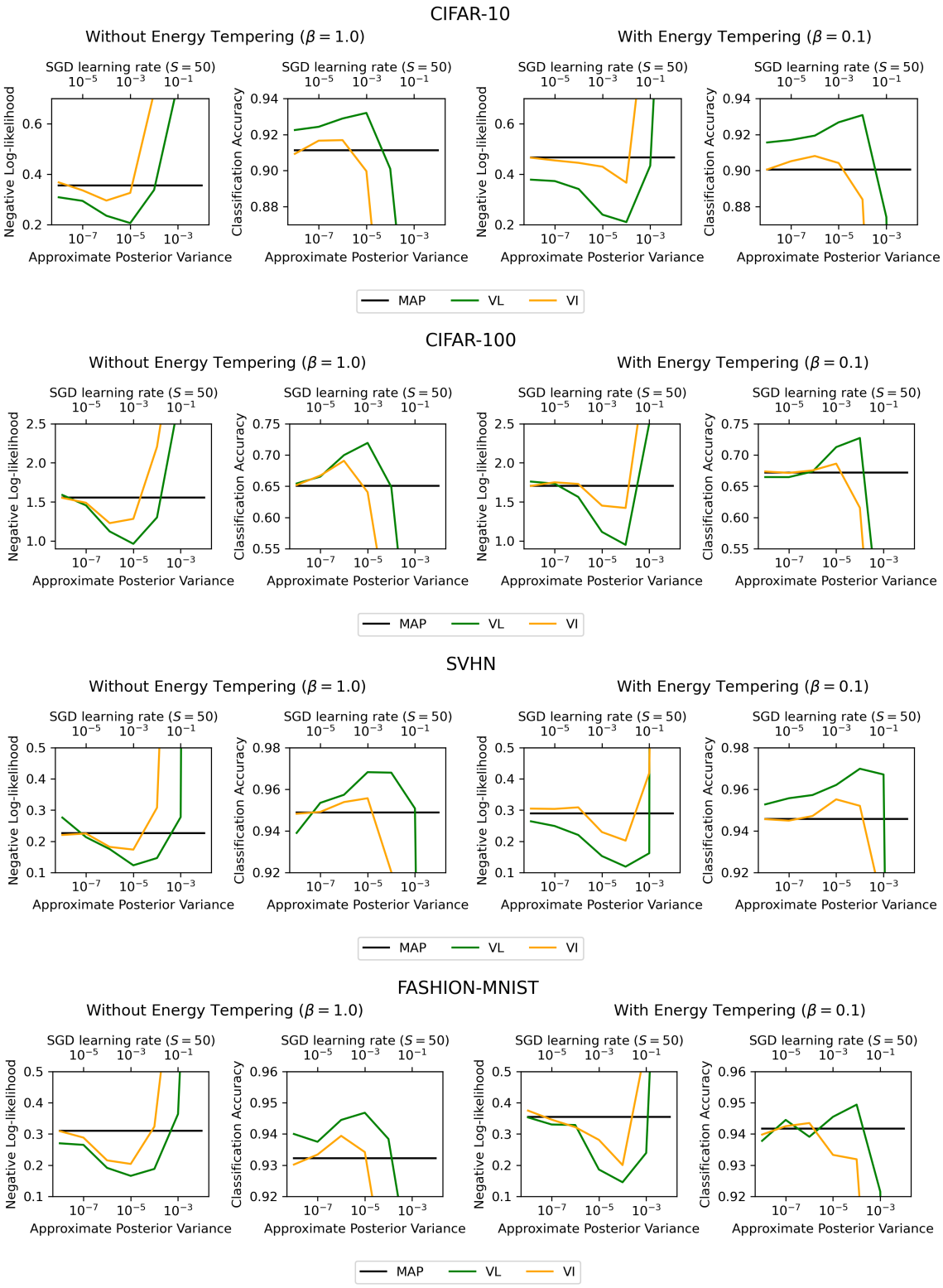

Figure 1. Training a PreactResNet-18 on various datasets with an fixed-variance approximate posterior, to mirror SGD. There are interesting connections between this approximate posterior and SGD, as the stationary distribution of SGD under a quadratic objective is a isotropic Gaussian with fixed variance controlled by the learning rate (App. B). As such, the posterior variance is shown on the lower x-axis and the corresponding value for the SGD learning rate is shown on the upper x-axis. "VI" corresponds to 200 training epochs.

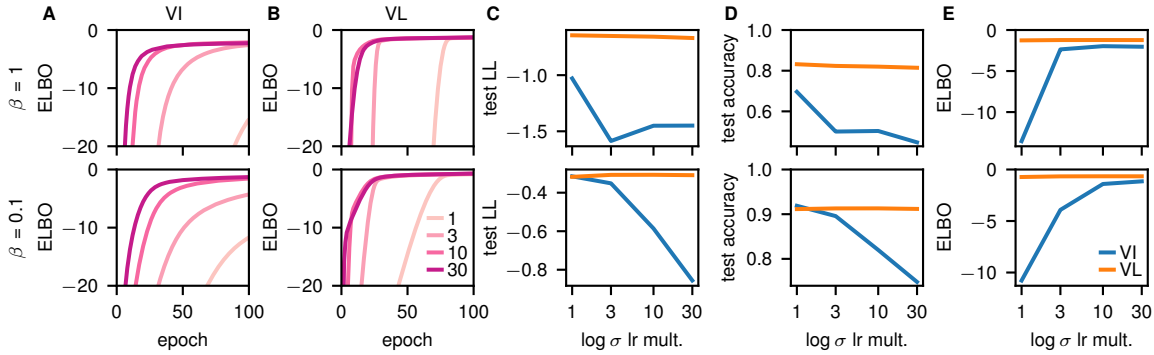

Figure 2. Analysis of early stopping in VI and VL. The first row is untempered ($\beta = 1$), and the second row is tempered ($\beta = 0.1$). **A** ELBO over epochs 0-100 (with the highest initial learning rate) for VI. Different lines correspond to networks with learning rate multipliers for $\log \sigma_\lambda$ of 1, 3, 10 and 30. **B** As **A**, but for VL. **CDE** Final test-log-likelihood (**C**), test accuracy (**D**) and ELBO (**E**) after 200 epochs for different learning rate multipliers.

Adam (Kingma & Ba, 2014) updates take the form,

$$\Delta\theta = \eta \frac{m}{\sqrt{v} + \epsilon} \tag{31}$$

where η is the learning rate, m is an unbiased estimator of the mean gradient, $\langle g \rangle$, v is an unbiased estimator of the squared gradient, $\langle g^2 \rangle$, and ϵ is a small positive constant to avoid divide-by-zero. The magnitude of the updates, $|\Delta\theta|$, is maximized by having exactly the same gradient on each step, in which case, neglecting ϵ, we have $|\Delta\theta| = \eta$. As such, with a learning rate of $\eta = 10^{-4}$, a training set of $50,000$ and a batch size of 128 parameters can move at most $50,000/128 \times 10^{-4} \approx 0.04$ per epoch. Doing 100 epochs at this learning rate, a parameter can change by at most 4 over the 100 epochs before the first learning rate step.

This is fine for the weights, which typically have very small values. However, the underlying parameters used for the variances typically take on larger values. In our case, we will use $\log \sigma_\lambda$ as the parameter, and initialize it to 3 less than the prior standard deviation, $\log s_\lambda - 3$. To ensure reasonable convergence, $\log \sigma_\lambda$ should be able to revert back to the prior, implying that it must be able to change by at least 3 during the course of training. Unfortunately, 3 is very close to the maximum possible change of 4, raising the possibility that the variance parameters will not actually converge. To check whether early-stopping was indeed an issue, we plotted the (tempered) ELBO for VI (Fig. 2A) and VL (Fig. 2B). For VI (Fig. 2A) with the standard setup (lightest line with a learning rate multiplier of 1), the ELBO clearly has not converged at 100 epochs, indicating early-stopping. Notably, this was far less of an issue with VL (Fig. 2B), and can be rectified by increasing the learning rate specifically for the $\log \sigma_\lambda$ parameters (darker lines).

We then plotted the test log-likelihood (Fig. 2C), test accuracy (Fig. 2D) and ELBO (Fig. 2E) against the learning rate multiplier. Again, the performance for VL (orange) was robust to changes in the learning rate multiplier. However, the performance of VI (blue) was very sensitive to the multiplier: as the multiplier increased, test performance fell but the ELBO rose. As we ultimately care about test performance, these results would suggest that we should use the lowest multiplier (1), and accept the possibility of early-stopping. That may be a perfectly good choice in many cases. However, VI is supposed to be an approximate Bayesian method, and using an alternative form for the ELBO,

$$\mathcal{L}_{\text{VI}} = \log \mathrm{P}\left(\mathbf{y}|\mathbf{x}\right) - D_{\text{KL}}\left(\mathrm{Q}\left(\mathbf{w}\right) || \, \mathrm{P}\left(\mathbf{w}|\mathbf{y}, \mathbf{x}\right)\right), \tag{32}$$

we can see that the ELBO measures KL-divergence between the true and approximate posterior, and hence the quality of our approximate Bayesian inference. As such, very poor ELBOs imply that the KL-divergence between the true and approximate posterior is very large, and hence the "approximate posterior" is no longer actually approximating the true posterior. As such, if we are to retain a Bayesian interpretation of VI, we need to use larger learning rate multipliers which give better values for the ELBO (Fig. 2E). However, in doing that, we get worse test performance (Fig. 2CD). This conflict between approximate posterior quality and test performance is very problematic: the Bayesian framework would suggest that as Bayesian inference becomes more accurate, performance should improve, whereas for VI, performance gets worse. Concretely, by initializing $\log \sigma_\lambda$ to a small value and then early-stopping, we leave $\log \sigma_\lambda$ at a small value through training, in which case VI becomes equivalent to MAP inference with a negligibly small amount of noise added to the weights. We would therefore expect early-stopped VI to behave (and be) very similar to MAP inference.

In subsequent experiments, we chose to use a learning rate multiplier of 10, as this largely eliminated early-stopping

Table 1. Performance of a PreactResNet-18 under VL and VI with a learned variances and MAP.

dataset	method	test log-like.	accuracy (%)	ECE
CIFAR-10	VL	**-0.31**	91.3	0.076
	VI	-0.59	82.0	0.065
	MAP	-0.38	**91.4**	0.055
	Wenzel et al. (2020)	-0.22	92.8	
CIFAR-100	VL	**-1.13**	**69.3**	0.123
	VI	-1.32	65.9	0.112
	MAP	-1.71	66.7	0.181
Fashion-MNIST	VL	**-0.18**	**94.2**	0.026
	VI	-0.24	92.4	0.032
	MAP	-0.37	**94.2**	0.044
SVHN	VL	**-0.13**	**97.2**	0.032
	VI	-0.17	96.3	0.020
	MAP	-0.24	95.4	0.026

(though see VI with $\beta = 0.1$; Fig. 2E).

5.3. Learned variance

Finally, we compared VL, VI and MAP in the setting where we allow the approximate posterior variances to be learned. In these experiments, we followed common practice by using a small degree of approximate posterior tempering, $\beta = 0.1$, (Wenzel et al., 2020), which is given a theoretical justification as accounting for the effects of data-curation in Aitchison (2020). In this setting, VL gave considerably better test-log-likelihoods than VI and MAP on all datasets tested (CIFAR-10, CIFAR-100, Fashion-MNIST and SVHN). VL always gave better test accuracies than VI, and was either better than or very close to MAP inference. As expected, previous approaches based on SGMCMC (Wenzel et al., 2020) gave slightly better performance, presumably because of the better posterior approximations and the use of an ensemble at test-time. As they did not actually try $\beta = 0.1$, we did a linear interpolation in the log-domain for the values they did obtain just above and just below 0.1.

While we evaluated the expected calibration error (ECE Naeini et al., 2015; Guo et al., 2017), the signal it gave was very confused, with MAP giving the best (lowest) value in CIFAR-10, VL giving the best value in Fashion-MNIST and VI giving the best value in CIFAR-100 and SVHN. Indeed, we believe that the test-log-likelihood itself is often a more relevant measure of uncertainty. In particular, the test-log-likelihood $\log \mathrm{P}\left(Y_i|X_i\right)$ will be large if the true label was assigned very low probability, and will continue to give increasingly large penalties for very small probabilities i.e. the penalty for moving from 0.1 to 0.01 is the same as from 0.01 to 0.001. This is especially relevant where there are some low-risk but very bad outcomes, (such as in self-driving cars), where it is often suggested that Bayesian neural networks should be applied. In contrast, the ECE bins predictive probabilities, and the bins are often quite large (e.g. from 0 to 0.1). The ECE is therefore unable to make strong distinctions between these low-probability predictions, instead focusing on "calibration" errors, which penalises e.g. predictions made with 60% probability only being correct 50% of the time. In high-risk settings such as self-driving cars, we care about small probabilities: if an action gives a 50% probability of crashing then obviously the car should not take that action, and changing that probability e.g. to 40% or 60% is highly unlikely to change the car's action. However, if an action gives a probability of crashing of 0.001%, then the car might take that action, and it might (eventually, or across enough cars) be catastrophic if the true probability of crashing in that setting is e.g. 1%. These differences are captured very effectively by the standard test-log-likelihood.

6. Conclusions

We gave a novel Variational Laplace approach to inference in Bayesian neural networks which combines the best of previous approaches based on Variational Inference and Laplace's Method. This method gave excellent empirical performance compared to VI.

References

Aitchison, L. A statistical theory of cold posteriors in deep neural networks. *arXiv preprint arXiv:2008.05912*, 2020.

Amato, F., López, A., Peña-Méndez, E. M., Vanhara, P., Hampl, A., and Havel, J. Artificial neural networks in medical diagnosis. *J Appl Biomed*, 11:47–58, 2013.

Azevedo-Filho, A. and Shachter, R. D. Laplace's method approximations for probabilistic inference in belief networks with continuous variables. In *Uncertainty Proceedings 1994*, pp. 28–36. Elsevier, 1994.

Barrett, D. G. and Dherin, B. Implicit gradient regularization. *arXiv preprint arXiv:2009.11162*, 2020.

Blundell, C., Cornebise, J., Kavukcuoglu, K., and Wierstra, D. Weight uncertainty in neural networks. *arXiv preprint arXiv:1505.05424*, 2015.

Bojarski, M., Del Testa, D., Dworakowski, D., Firner, B., Flepp, B., Goyal, P., Jackel, L. D., Monfort, M., Muller, U., Zhang, J., et al. End to end learning for self-driving cars. *arXiv preprint arXiv:1604.07316*, 2016.

Daunizeau, J. The variational laplace approach to approximate bayesian inference. *arXiv preprint arXiv:1703.02089*, 2017.

Daunizeau, J., Friston, K. J., and Kiebel, S. J. Variational bayesian identification and prediction of stochastic nonlinear dynamic causal models. *Physica D: nonlinear phenomena*, 238(21):2089–2118, 2009.

Friston, K., Mattout, J., Trujillo-Barreto, N., Ashburner, J., and Penny, W. Variational free energy and the laplace approximation. *Neuroimage*, 34(1):220–234, 2007.

Guo, C., Pleiss, G., Sun, Y., and Weinberger, K. Q. On calibration of modern neural networks. In *International Conference on Machine Learning*, pp. 1321–1330. PMLR, 2017.

He, K., Zhang, X., Ren, S., and Sun, J. Identity mappings in deep residual networks. In *European conference on computer vision*, pp. 630–645. Springer, 2016.

Huang, C.-W., Tan, S., Lacoste, A., and Courville, A. C. Improving explorability in variational inference with annealed variational objectives. In *Advances in Neural Information Processing Systems*, pp. 9701–9711, 2018.

Kingma, D. P. and Ba, J. Adam: A method for stochastic optimization. *arXiv preprint arXiv:1412.6980*, 2014.

Kingma, D. P. and Welling, M. Auto-encoding variational bayes. *arXiv preprint arXiv:1312.6114*, 2013.

Kunstner, F., Hennig, P., and Balles, L. Limitations of the empirical fisher approximation for natural gradient descent. In *Advances in Neural Information Processing Systems*, pp. 4156–4167, 2019.

MacKay, D. J. *Information theory, inference and learning algorithms*. Cambridge university press, 2003.

Malinin, A., Mlodozeniec, B., and Gales, M. Ensemble distribution distillation. *arXiv preprint arXiv:1905.00076*, 2019.

Mandt, S., Hoffman, M. D., and Blei, D. M. Stochastic gradient descent as approximate bayesian inference. *The Journal of Machine Learning Research*, 18(1):4873–4907, 2017.

McAllister, R., Gal, Y., Kendall, A., Van Der Wilk, M., Shah, A., Cipolla, R., and Weller, A. Concrete problems for autonomous vehicle safety: Advantages of bayesian deep learning. In *International Joint Conferences on Artificial Intelligence, Inc.*, 2017.

Naeini, M. P., Cooper, G., and Hauskrecht, M. Obtaining well calibrated probabilities using bayesian binning. In *Proceedings of the AAAI Conference on Artificial Intelligence*, 2015.

Neyshabur, B., Bhojanapalli, S., McAllester, D., and Srebro, N. Exploring generalization in deep learning. In *Advances in neural information processing systems*, pp. 5947–5956, 2017.

Ober, S. W. and Aitchison, L. Global inducing point variational posteriors for bayesian neural networks and deep gaussian processes, 2020.

Rezende, D. J., Mohamed, S., and Wierstra, D. Stochastic backpropagation and approximate inference in deep generative models. *arXiv preprint arXiv:1401.4082*, 2014.

Ritter, H., Botev, A., and Barber, D. A scalable laplace approximation for neural networks. In *6th International Conference on Learning Representations, ICLR 2018-Conference Track Proceedings*, volume 6. International Conference on Representation Learning, 2018.

Smith, S. L., Dherin, B., Barrett, D. G., and De, S. On the origin of implicit regularization in stochastic gradient descent. *arXiv preprint arXiv:2101.12176*, 2021.

Wainwright, M. J. and Jordan, M. I. *Graphical models, exponential families, and variational inference*. Now Publishers Inc, 2008.

Welling, M. and Teh, Y. W. Bayesian learning via stochastic gradient langevin dynamics. In *Proceedings of the 28th international conference on machine learning (ICML-11)*, pp. 681–688, 2011.

Wenzel, F., Roth, K., Veeling, B. S., Swiatkowski, J., Tran, L., Mandt, S., Snoek, J., Salimans, T., Jenatton, R., and Nowozin, S. How good is the Bayes posterior in deep

neural networks really? *arXiv preprint arXiv:2002.02405*, 2020.

Wu, A., Nowozin, S., Meeds, E., Turner, R. E., Hernández-Lobato, J. M., and Gaunt, A. L. Deterministic variational inference for robust bayesian neural networks. *arXiv preprint arXiv:1810.03958*, 2018.

A. Variational Inference for Bayesian Neural Networks

We need to optimize the expectation in Eq. (4) with respect to parameters of $\mathrm{Q}(\mathbf{w})$, the distribution over which the expectation is taken. We therefore use the reparameterisation trick (Kingma & Welling, 2013; Rezende et al., 2014) — we write $\mathbf{w}$ in terms of $\boldsymbol{\epsilon}$,

$$w_\lambda(\epsilon_\lambda) = \mu_\lambda + \sigma_\lambda \epsilon_\lambda \tag{33}$$

where $\epsilon_\lambda \sim \mathcal{N}(0,1)$. Thus, the ELBO can be written as an expectation over $\boldsymbol{\epsilon}$,

$$\mathcal{L}_{\mathrm{VI}} = \mathop{\mathbb{E}}_{\boldsymbol{\epsilon}}\left[\sum_i \log \mathrm{P}\left(y_i|x_i,\mathbf{w}(\boldsymbol{\epsilon})\right) + \sum_\lambda \log \frac{\log \mathrm{P}\left(w_\lambda(\epsilon_\lambda)\right)}{\log \mathrm{Q}\left(w_\lambda(\epsilon_\lambda)\right)}\right]. \tag{34}$$

where the distribution over $\boldsymbol{\epsilon}$ is now fixed. Critically, now the expected gradient of the term inside the expectation is equal to the gradient of $\mathcal{L}_{\mathrm{VI}}$, so we can use samples of $\boldsymbol{\epsilon}$ to estimate the expectation.

B. The Stationary Distribution of SGD

We sought to relate these gradient regularizers back to work on SGD (Barrett & Dherin, 2020). In particular, we looked to work on the stationary distribution of SGD, which noted that under quadratic losses functions, SGD samples an *isotropic* Gaussian (i.e. with covariance proportional to the identity matrix). In particular, consider a loss function which is locally closely approximated by a quadratic. Without loss of generality, we consider a mode at $\mathbf{w} = \mathbf{0}$,

$$\log \mathrm{P}\left(\{y_i\}_{i=1}^P | \{x_i\}_{i=1}^P, \mathbf{w}\right) = -\tfrac{P}{2}\mathbf{w}^T\mathbf{H}\mathbf{w} + \mathrm{const}\,. \tag{35}$$

where P is the total number of datapoints. Typically, the objective used in SGD is the loss for a minibatch of size S_{SGD}. Following Mandt et al. (2017), we use the Fisher Information to identify the noise in the minibatch gradient,

$$\frac{\partial}{\partial \mathbf{w}}\left[\tfrac{1}{S_{\mathrm{SGD}}} \log \mathrm{P}\left(\mathbf{y}_j|x_j,\mathbf{w}\right)\right] = -\mathbf{H}\mathbf{w} + \tfrac{1}{\sqrt{S_{\mathrm{SGD}}}}\mathbf{H}^{1/2}\boldsymbol{\xi}(t), \tag{36}$$

where $\boldsymbol{\xi}(t)$ is sampled from a standard IID Gaussian. For SGD, this gradient is multiplied by a learning rate, η_{SGD},

$$\mathbf{w}(t+1) = \mathbf{w}(t) - \eta_{\mathrm{SGD}}\mathbf{H}\mathbf{w}(t) + \tfrac{\eta_{\mathrm{SGD}}}{\sqrt{S_{\mathrm{SGD}}}}\mathbf{H}^{1/2}\boldsymbol{\xi}(t), \tag{37}$$

This is an multivariate Gaussian autoregressive process, so we can solve for the stationary distribution of the weights. In particular, we note that the covariance at time $t+1$ is

$$\begin{aligned}
\mathbb{C}\left[\mathbf{w}\left(t+1\right)\right] &= \mathbb{E}\left[\left(\mathbf{w}(t) - \eta_{\mathrm{SGD}}\mathbf{H}\mathbf{w}(t) - \tfrac{\eta_{\mathrm{SGD}}}{\sqrt{S_{\mathrm{SGD}}}}\mathbf{H}^{1/2}\boldsymbol{\xi}(t)\right)^T\left(\mathbf{w}(t) - \eta_{\mathrm{SGD}}\mathbf{H}\mathbf{w}(t) - \tfrac{\eta_{\mathrm{SGD}}}{\sqrt{S_{\mathrm{SGD}}}}\mathbf{H}^{1/2}\boldsymbol{\xi}(t)\right)\right] \\
\mathbb{C}\left[\mathbf{w}\left(t+1\right)\right] &= \left(\mathbf{I} - \eta_{\mathrm{SGD}}\mathbf{H}\right)^T\mathbb{C}\left[\mathbf{w}(t)\right]\left(\mathbf{I} - \eta_{\mathrm{SGD}}\mathbf{H}\right) + \tfrac{\eta_{\mathrm{SGD}}^2}{S_{\mathrm{SGD}}}\mathbf{H}
\end{aligned} \tag{38}$$

Following Mandt et al. (2017), when the learning rate is small, the quadratic term can be neglected.

$$\mathbb{C}\left[\mathbf{w}\left(t+1\right)\right] \approx \mathbb{C}\left[\mathbf{w}(t)\right] - \eta_{\mathrm{SGD}}\mathbf{H}\,\mathbb{C}\left[\mathbf{w}(t)\right] - \eta_{\mathrm{SGD}}\,\mathbb{C}\left[\mathbf{w}(t)\right]\mathbf{H} + \tfrac{\eta_{\mathrm{SGD}}^2}{S_{\mathrm{SGD}}}\mathbf{H} \tag{39}$$

We then solve for steady-state in which $\boldsymbol{\Sigma} = \mathbb{C}\left[\mathbf{w}(t+1)\right] = \mathbb{C}\left[\mathbf{w}(t)\right]$,

$$0 \approx -\eta_{\mathrm{SGD}}\left(\mathbf{H}^T\boldsymbol{\Sigma}_{\mathrm{SGD}} + \boldsymbol{\Sigma}_{\mathrm{SGD}}\mathbf{H}\right) + \tfrac{\eta_{\mathrm{SGD}}^2}{S_{\mathrm{SGD}}}\mathbf{H} \tag{40}$$

so,

$$\boldsymbol{\Sigma} \approx \tfrac{\eta_{\mathrm{SGD}}}{2S_{\mathrm{SGD}}}\mathbf{I}. \tag{41}$$

We therefore considered a family of approximate posteriors matching these stationary distributions, by setting all variances, σ_λ^2, to a single, fixed value, $\frac{\eta_{\mathrm{SGD}}}{2S_{\mathrm{SGD}}}$.

C. Runtime

The runtime of the methods is listed in Table 2. While VL is relatively slow due to the need to compute second-derivatives, it is still eminently feasible. Furthermore, we did not find that increasing the number of epochs improved performance either for VI or MAP as we are already training to convergence.

Table 2. Time per epoch for different methods on CIFAR-10

method	time per epoch (s)
VL	114.9
VI	43.2
MAP	41.8